JCI insight

IL-33–mediated IL-13 secretion by ST2$^+$ Tregs controls inflammation after lung injury

Quan Liu, … , Timothy R. Billiar, Hēth R. Turnquist

JCI Insight. 2019;4(6):e123919. https://doi.org/10.1172/jci.insight.123919.

Research Article | Immunology | Pulmonology

Graphical abstract

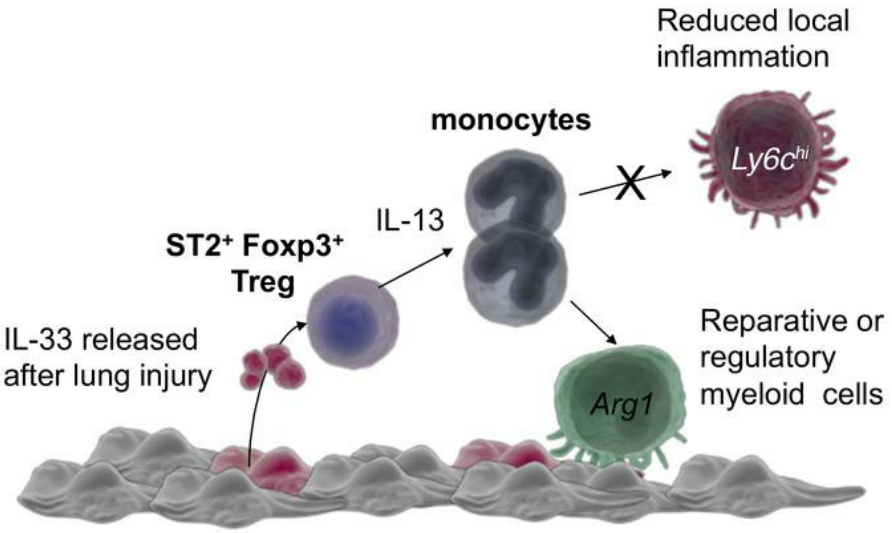

JCI insight

RESEARCH ARTICLE

IL-33–mediated IL-13 secretion by ST2$^+$ Tregs controls inflammation after lung injury

Quan Liu,[1,2,3] Gaelen K. Dwyer,[1,4] Yifei Zhao,[1,5] Huihua Li,[6] Lisa R. Mathews,[1] Anish Bhaswanth Chakka,[7] Uma R. Chandran,[7] Jake A. Demetris,[1,8] John F. Alcorn,[9] Keven M. Robinson,[7] Luis A. Ortiz,[10] Bruce R. Pitt,[10] Angus W. Thomson,[1,2,4] Ming-Hui Fan,[6] Timothy R. Billiar,[2] and Hēth R. Turnquist[1,2,4]

[1]Thomas E. Starzl Transplantation Institute, [2]Department of Surgery, University of Pittsburgh School of Medicine, Pittsburgh, Pennsylvania, USA. [3]Southern University of Science and Technology School of Medicine, Shenzhen, China. [4]Department of Immunology, University of Pittsburgh School of Medicine, Pittsburgh, Pennsylvania, USA. [5]Tsinghua University School of Medicine, Beijing, China. [6]Division of Pulmonary, Allergy, and Critical Care Medicine, Department of Medicine, [7]Department of Biomedical Informatics, and [8]Department of Pathology, University of Pittsburgh School of Medicine, Pittsburgh, Pennsylvania, USA. [9]Department of Pediatrics, University of Pittsburgh Medical Center Children's Hospital of Pittsburgh, Pittsburgh, Pennsylvania, USA. [10]Department of Environmental and Occupational Heath, University of Pittsburgh Graduate School of Public Health, Pittsburgh, Pennsylvania, USA.

Acute respiratory distress syndrome is an often fatal disease that develops after acute lung injury and trauma. How released tissue damage signals, or alarmins, orchestrate early inflammatory events is poorly understood. Herein we reveal that IL-33, an alarmin sequestered in the lung epithelium, is required to limit inflammation after injury due to an unappreciated capacity to mediate Foxp3$^+$ Treg control of local cytokines and myeloid populations. Specifically, *Il33*$^{-/-}$ mice are more susceptible to lung damage–associated morbidity and mortality that is typified by augmented levels of the proinflammatory cytokines and Ly6C^{hi} monocytes in the bronchoalveolar lavage fluid. Local delivery of IL-33 at the time of injury is protective but requires the presence of Treg cells. IL-33 stimulates both mouse and human Tregs to secrete IL-13. Using *Foxp3*^{Cre} × *Il4*/*Il13*$^{fl/fl}$ mice, we show that Treg expression of IL-13 is required to prevent mortality after acute lung injury by controlling local levels of G-CSF, IL-6, and MCP-1 and inhibiting accumulation of Ly6C^{hi} monocytes. Our study identifies a regulatory mechanism involving IL-33 and Treg secretion of IL-13 in response to tissue damage that is instrumental in limiting local inflammatory responses and may shape the myeloid compartment after lung injury.

Introduction

Acute lung injury (ALI) can result from direct injury caused by bacterial or viral pneumonia, aspiration, and toxin inhalation and indirect injury following sepsis, major trauma, and blood transfusion (1, 2). ALI may lead to the more severe acute respiratory distress syndrome (ARDS) that has a complex pathology and causes considerable morbidity and mortality (3, 4). Diffuse alveolar damage, pulmonary edema, and hypoxemia due to dysregulated inflammation, reflected by increased inflammatory cytokines in the plasma or bronchoalveolar lavage fluid (BALF) and accumulation of extravascular neutrophils, are defining features of ARDS (2, 5). In addition to neutrophils, macrophages and monocytes also play a causal role in ARDS, as they initiate and perpetuate lung damage through contributing to the local inflammation that causes increased epithelial and endothelial permeability (6–8). Despite intensive basic and clinical study over the past several decades, there remains a lack of effective treatments to prevent or resolve ARDS (2, 9–17). Thus, the risk of mortality remains high for ARDS patients (4, 18). Lung-protective mechanical ventilation and conservative fluid management reduce inflammatory cytokine levels and neutrophil numbers in the BALF of animals subjected to ALI and ALI/ARDS patients (19, 20). To date, these supportive procedures that reduce early inflammation are the only means to provide consistent improvement in patient outcome (4, 18).

Authorship note: QL and GKD are co–first authors.

Conflict of interest: The authors have declared that no conflict of interest exists.

Submitted: July 31, 2018
Accepted: February 12, 2019
Published: February 19, 2019

Reference information:
JCI Insight. 2019;4(6):e123919.
https://doi.org/10.1172/jci.insight.123919.

The pathophysiology of ALI is commonly studied in rodent models where instillation of chemicals, such as bleomycin, damages the epithelial and endothelial barriers, thus increasing alveolar-capillary permeability that results in fluid and protein accumulation in the alveolus (21–24). The BALF isolated in the first several days of bleomycin-induced ALI contains high levels of neutrophils and inflammatory cytokines, including IL-1β, IL-6, TNF, and monocyte chemoattractant protein 1 (MCP-1)/CCL2 (22, 23, 25). Infiltrating inflammatory monocytes, monocyte-derived interstitial macrophages, and residential alveolar macrophages (AMs) are present and thought to contribute to the early inflammatory response and tissue damage after experimental ALI, including that induced by bleomycin (6, 26). These same cells, however, also participate in inflammation and injury resolution, as well as the development of subsequent fibrotic disease after ALI (6, 27, 28). Foxp3$^+$ Tregs have also been implicated in the resolution of ALI by shaping alveolar cytokines, potentially by modulating those produced by macrophages (29). Recently, Misharin et al. revealed that the primary drivers of lung fibrosis following tissue injury are monocyte-derived AMs that rapidly replace depleted fetus-derived tissue-resident AMs after bleomycin (30). Gaining an understanding of the endogenous mechanisms controlling early inflammation and shifting the local environment, including resident and infiltrating myeloid cells, away from an inflammatory state and towards one of rapid resolution and effective repair after ALI could lead to novel therapies that can prevent or rapidly resolve ALI/ARDS, as well as reduce subsequent fibrosis.

Tissue injury associated with trauma leads to the release of alarmins, or self-molecules that alert the immune system to damage (31–34). One alarmin of particular interest is IL-33, which is highly expressed in the lungs of mice and humans (35). While IL-33 supports inflammatory responses to parasites, it also drives allergic airway disease and fibrosis of the lung and other organs (35–39). However, Tregs that express the IL-33 receptor, serum stimulation-2 (ST2, encoded by *Il1rl1*), upregulate amphiregulin after IL-33 stimulation and this mechanism has been implicated recently in epithelial tissue repair after viral infection of the lung (40). Related in vitro studies have suggested that IL-33 potentiates the suppressive capacity of Tregs (41). After muscle injury, the presence of ST2$^+$ Tregs have been associated with the transition of infiltrating myeloid cells from a proinflammatory subset to a reparative/regenerative subset (42). Mechanisms by which IL-33 stimulation of ST2$^+$ Tregs contributes to local control of myeloid cell function or differentiation, however, are unknown. These studies proposing the regulatory or reparative activity of IL-33 are in direct contrast to other investigations that suggest IL-33 causes functional dysregulation in Tregs in the lung (43) and skin (44). This dysregulation is associated with the lost capacity to suppress (Teff) T cell proliferation and pathological induction of type 2 cytokine production (43, 44). Accordingly, the role of IL-33 in acute organ injury is unclear and the mechanisms, especially involving Tregs, by which IL-33 may shape early inflammation or contribute to injury resolution are poorly defined.

The goal of the current studies was to establish how IL-33 impacts Tregs after bleomycin-induced ALI and to ascertain the role that this interaction plays in shaping the early inflammatory environment. In doing this, we made the unanticipated discovery that IL-33 is critical to prevent mortality after ALI by controlling the early inflammatory response after tissue injury through its actions on Tregs. Mice deficient in IL-33 were found to be more susceptible to lung damage–associated lethality, which is typified by augmented levels of inflammatory cytokines and immune cell infiltration. We then established that the mechanism underlying IL-33 control of the local inflammatory immune response after ALI involves the induction of IL-13 production by ST2$^+$ Tregs that served to limit local inflammatory cytokines and the presence of inflammatory myeloid cells. In total, we establish an important protective and immunoregulatory capacity of IL-13 and IL-33 after lung injury that supports resolution of the inflammation associated with ALI. Given that inflammatory responses are considered primary drivers of ARDS, IL-13, IL-33, or IL-33–stimulated Tregs secreting IL-13 may be novel therapeutic targets to further evaluate early after ALI.

Results

IL-33 deficiency results in an impaired ability to survive ALI induced by bleomycin. Augmenting IL-33 in IL-33–replete mice via delivery of the recombinant (r) protein or inducing overexpression by adenoviral vectors has been suggested to augment the development of fibrosis after bleomycin administration (45, 46). Yet the impact of endogenous IL-33 after bleomycin-induced ALI is poorly understood. When compared with wild-type (WT) mice after intratracheal (i.t.) bleomycin-induced chemical ALI, *Il33*$^{-/-}$ mice exhibited a more substantial loss of body weight (Figure 1A) and the lack of IL-33 accelerated the death of *Il33*$^{-/-}$ mice (Figure 1B) compared with WT. Histological examination revealed that the reduced survival of *Il33*$^{-/-}$ mice

was associated with increased lung pathology and inflammation (Figure 1C). Histology scored on day 7 following i.t. bleomycin revealed that *Il33*$^{-/-}$ mice had significant increases in perivascular and peribronchiolar inflammation (Figure 1, C and D). Likewise, lungs from *Il33*$^{-/-}$ mice had markedly increased levels of intra-AM infiltration and early fibrosis compared with WT mice (Figure 1, C and D). Computerized calculation of total lung consolidation suggested a more significant loss of functional lung area in *Il33*$^{-/-}$ mice (Figure 1D). IL-33–deficient mice also displayed a slight trend towards increased levels of total protein in BALF at days 7–8 after bleomycin (Supplemental Figure 1A; supplemental material available online with this article; https://doi.org/10.1172/jci.insight.123919DS1). Surviving *Il33*$^{-/-}$ mice on day 13 also displayed increased levels of hydroxyproline that was consistent with the early increase in fibrosis identified by histopathology (Figure 1, C and D, and Supplemental Figure 1B). Together, these data suggest a role for endogenous IL-33 in the protection of mice from mortality after bleomycin-induced ALI. Also, as the course of the immune response to bleomycin injury to the lung is well studied and described, it was apparent that IL-33–deficient mice were dying during the peak of the inflammatory immune response (47, 48).

Evidence for increased inflammation after ALI in the absence of IL-33. We next verified that restoration of IL-33 could protect *Il33*$^{-/-}$ mice from early mortality following bleomycin challenge. While a one-time instillation of rIL-33 at the time of 1.5 IU/kg i.t. bleomycin did not rescue *Il33*$^{-/-}$ mice (data not shown), rIL-33 treatment did rescue a significant percentage of mice from mortality after 1.0 IU/kg bleomycin-induced lung injury (Figure 2A). At this dose of bleomycin, *Il33*$^{-/-}$ mice again displayed an accelerated death rate relative to WT mice (Figure 2A).

Given the apparent failure of *Il33*$^{-/-}$ mice to control or resolve the inflammatory response after injury, we next sought to define how restoration of IL-33 altered the local immune and cytokine environment early after bleomycin-induced lung injury. Luminex quantification of BALF cytokines revealed that IL-33 was a negative regulator of IL-6, granulocyte colony-stimulating factor (G-CSF), MCP1/CCL2, leukemia inhibitory factor (LIF), and IL-1α in samples collected on days 7 and 8 after bleomycin insult (Figure 2B). While detected, we did not observe significant differences between WT and *Il33*$^{-/-}$ BALF levels of Eotaxin/CCL11, IL-5, IL-9, CXCL10, CXCL1, and CXCL9 (data not shown). Granulocyte-macrophage colony-stimulating factor (GM-CSF), IFN-γ, IL-1β, IL-2, IL-3, IL-4, IL-7, IL-10, IL-12p40, IL-12p70, IL-13, IL-15, IL-17, and CXCL5 were not detected in the BALF at this time point (data not shown).

When the cellular infiltrates present in the BALF of *Il33*$^{-/-}$ mice at day 7 and 8 after bleomycin were compared to that of WT by flow cytometry, it was found that the BALF of *Il33*$^{-/-}$ mice had significantly increased frequency of neutrophils (CD45^{+}CD11b^{hi}Siglec-F^{-}Ly6G^{hi}; Figure 2, C and D, and Supplemental Figure 2). Intratracheal delivery of rIL-33 to *Il33*$^{-/-}$ mice reduced the frequency and total number of neutrophils to WT levels, implicating the importance of IL-33 as a critical regulator of early neutrophil infiltration during ALI (Figure 2C and Supplemental Figure 2C). While we did not see a significant difference between WT and *IL33*$^{-/-}$ mice in the anticipated loss of AMs (CD45^{+}CD11b^{lo}Siglec-F^{hi}) after bleomycin instillation, we did find that rIL-33 delivery limited the loss of this immune population (Figure 2C). We did not find any consistent alteration in the frequency or number of eosinophils (CD45^{+}CD11b^{+}Ly6G^{lo}Siglec-F^{+}) between any of the groups (data not shown). IL-33–deficient mice did, however, display a trend towards increased frequency of Ly6C^{hi} inflammatory monocytes (CD45^{+}CD11b^{hi}CD11c^{lo}Ly6C^{hi}) in BALF 7 or 8 days after bleomycin treatment, which was reversed by IL-33 delivery (Figure 2D). An increase in Ly6C^{lo} monocyte frequency relative to that of Ly6C^{hi} monocytes in sites of injury is correlated with tissue repair and inflammation resolution (28, 42, 49). Interestingly, delivery of IL-33 at the time of bleomycin insult potently increased the frequency, but not total number, of Ly6C^{lo} monocytes in the BALF (Figure 2D and Supplemental Figure 2C). Our data generated on day 7 and 8 after bleomycin injury are consistent with IL-33 acting as a crucial local factor that limits and qualitatively shapes the early inflammatory response after ALI.

IL-33 protective function following ALI is mediated by Tregs. Accumulation of Tregs expressing ST2 has been implicated in muscle repair after skeletal injury and this phenomenon was differentially regulated by the availability of local IL-33 (50). Thus, we first examined whether a decrease in the baseline level of Tregs, including the ST2^{+} subset, due to a loss of IL-33 in the normal lung, could account for the observed increase in mortality of *Il33*$^{-/-}$ mice after bleomycin. Our analysis, however, established that the frequency of Tregs in CD45^{+} lymphocytes isolated from the lung parenchyma of normal and *Il33*$^{-/-}$ mice was not significantly different, indicating *Il33*$^{-/-}$ mice did not have a baseline deficiency in Tregs (Supplemental Figure 3, A and B). We also established that a lack of IL-33 did not significantly reduce the frequency of interstitial Tregs at day 8 after bleomycin delivery relative to WT lungs, although delivery of rIL-33

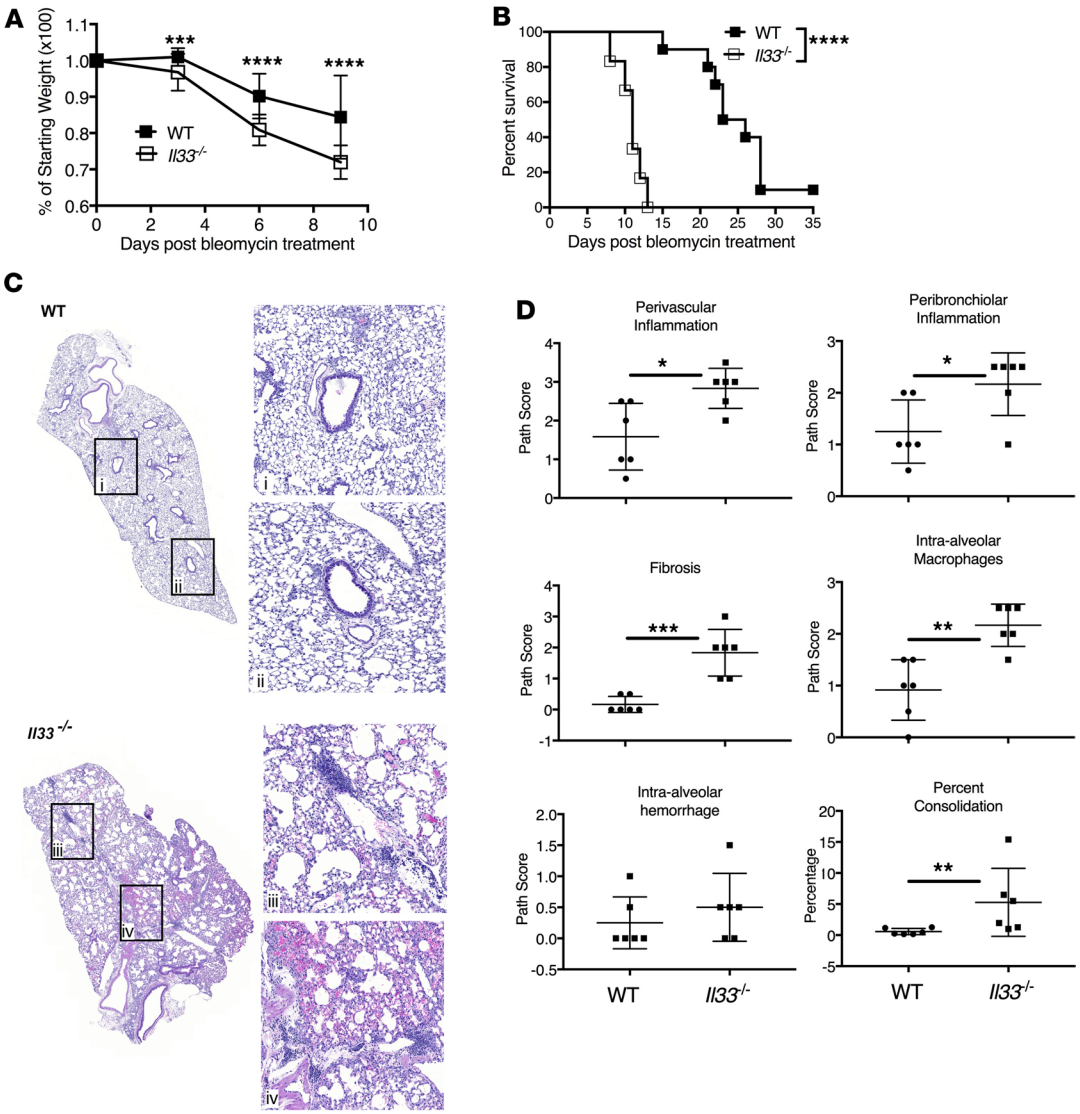

Figure 1. IL-33 deficiency increases mortality after chemically induced acute lung injury (ALI). (**A**) Weight loss and (**B**) mortality rate of WT and *Il33*$^{-/-}$ B6 mice injected intratracheally (i.t.) with bleomycin (1.5 IU/kg). Data depicted are representative of 2 independent experiments (n = 6–10 mice per group). (**C**) Representative hematoxylin and eosin (H&E) staining of lung sections from WT and *Il33*$^{-/-}$ mice at day 7 after 1.5 IU/kg bleomycin i.t. delivery. (**D**) Scoring of H&E–stained lung sections collected at day 7 after bleomycin administration for perivascular and peribronchiolar inflammation, fibrosis, intra-alveolar macrophages and hemorrhage, and consolidated parenchyma. Data depicted are from 2 pooled experiments and representative of 3 experiments completed (n = 6 mice per group). Data are the mean ± SD. P values were determined by 2-tailed Student's t test (**A** and **D**), log-rank test (**B**), or Mann-Whitney test (**D**, "percent consolidation"). *$P < 0.05$; **$P < 0.01$; ***$P < 0.001$; ****$P < 0.0001$.

increased the frequency of ST2$^+$ Tregs in the lung (Figure 3, A and B). A similar phenotype was observed for type 2 innate lymphoid cells (ILC2s; CD45$^+$Lineage$^-$ICOS$^+$Sca-1$^+$) following bleomycin challenge, as the frequency of ILC2s was not reduced in *Il33*$^{-/-}$ mice after bleomycin-induced ALI but was increased by local rIL-33 delivery (Supplemental Figure 4).

We have previously shown that rIL-33 delivery expands ST2$^+$ Tregs to promote heart allograft survival (51) or prevent graft-versus-host disease (GVHD) (52) in a Treg-dependent manner. To better establish if the observed protective capacity of IL-33 after lung injury depended on Tregs or ILC2s, we utilized *Foxp3*^{DTR} B6 mice that permit diphtheria toxin (DT) depletion of Tregs due to their *Foxp3* promoter–driven expression of the DT receptor (53). The use of this model would, however, leave ILC2s intact. Importantly, we found that rIL-33 delivery with bleomycin to Treg-replete *Foxp3*^{DTR} B6 mice provided significant protection relative to Treg-replete *Foxp3*^{DTR} B6 mice receiving bleomycin alone (Figure 3C). Thus, we demonstrated the protective capacity of local IL-33 against bleomycin-induced ALI in a second strain combination. We also verified

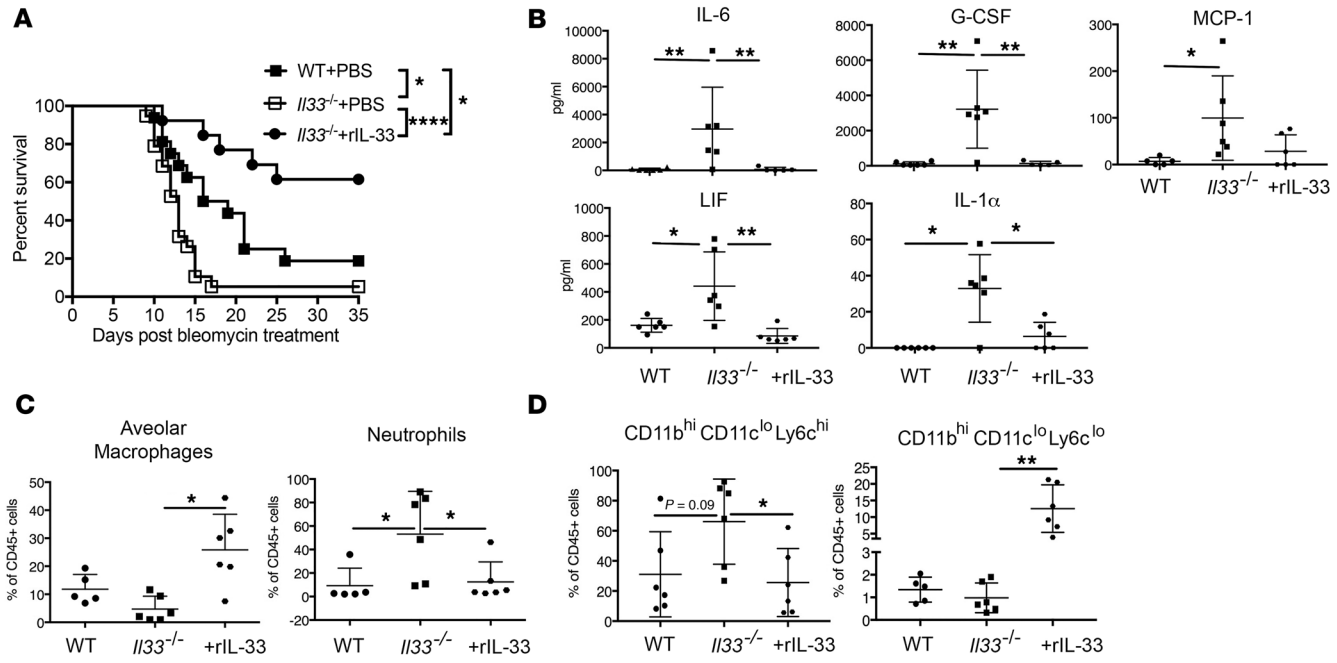

Figure 2. Local delivery of IL-33 protects *Il33*$^{-/-}$ mice from mortality after ALI and reduces the frequency of proinflammatory cytokines and myeloid cells in alveoli. (**A**) Survival of WT or *IL33*$^{-/-}$ B6 mice injected i.t. with 1.0 IU/kg bleomycin alone or with 1 μg rIL-33. Data are from 2 pooled experiments. (**B**) At days 7–8 after bleomycin delivery, bronchoalveolar lavage fluid (BALF) from *Il33*$^{-/-}$ mice had increased IL-6, G-CSF, LIF, IL-1α, and MCP-1 concentrations, which were significantly reduced by rIL-33 restoration. Data are from 1 experiment representative of 2, and n = 5–6 mice per group. (**C** and **D**) Flow cytometric assessment of BALF cells from WT and *Il33*$^{-/-}$ treated as in **A**. (**C**) Frequencies of alveolar macrophages (CD45$^+$CD11b^{lo}Siglec-F$^+$) and neutrophils (CD45$^+$CD11b^{hi}Siglec-F$^-$Ly6G^{hi}). (**D**) Frequencies of alveolar Ly6C^{hi} inflammatory monocytes (CD45$^+$CD11b^{hi}CD11c^{lo}Ly6C^{hi}) and Ly6C^{lo} immunosuppressive and reparative monocytes (CD45$^+$CD11b^{hi}CD11c^{lo}Ly6C^{lo}). Data are representative of 2 independent experiments, with 5–6 mice per group in each experiment. Data are the mean ± SD. P values were determined by log-rank test (**A**), or 1-way ANOVA followed by Tukey's multiple comparisons test (**B**–**D**). *P < 0.05; **P < 0.01.

that there were comparable rates of DT-mediated depletion between mice treated with IL-33 and those left untreated (Supplemental Figure 5). As expected (29), Treg-depleted mice display increased susceptibility to death after bleomycin compared with Treg-replete mice (Figure 3C). IL-33–treated, Treg-depleted mice had a slight, but nonsignificant increase in survival after i.t. bleomycin, suggesting a minimal role for ILC2s in IL-33–mediated protection early after ALI. In total, these data support the importance of IL-33 action on Tregs for a protective function following ALI.

IL-33 stimulates the secretion of IL-13 by murine ST2$^+$ Tregs. IL-33 can directly support the expansion of ST2$^+$ Tregs via activation of the p38 pathway (52) and IL-33 support of Treg accumulation is implicated in their function in muscle repair (50) and protection against GVHD (52). We have established previously that this subset of Tregs is suppressive in standard ex vivo Treg suppression assays (51, 54). We next used RNA sequencing (RNA-Seq) to define how else IL-33 may impact Tregs by assessing the expression signature of IL-33–stimulated ST2$^+$ Tregs compared with that of untreated ST2$^+$ Tregs (Figure 4A). These data revealed that ST2$^+$ Tregs stimulated with rIL-33 for 6 hours exhibited increased expression of *Il10*, as expected (55), but also exhibited increased *Il13* compared with unstimulated ST2$^+$ Tregs (Figure 4A). We confirmed the transcriptional upregulation of *Il10* and *Il13* in ex vivo–sorted ST2$^+$ and ST2$^-$ Tregs from rIL-33–treated and PBS-treated mice via qPCR (Figure 4B). We next utilized Foxp3$^+$ reporter mice to characterize the cytokine production induced by IL-33 in ST2$^+$ Tregs relative to other CD4$^+$ T cells. As shown in Figure 4C, splenic CD4$^+$ T cells could be sorted into 4 populations based on their expression of CD25, Foxp3, and ST2. These populations were Th2 cells (CD4$^+$CD25^{hi}ST2$^+$Foxp3$^-$), CD25^{lo}Foxp3$^+$ T cells (CD4$^+$CD25^{lo}ST2$^-$Foxp3$^+$), ST2$^+$ Tregs (CD4$^+$CD25^{hi}ST2$^+$Foxp3$^+$), and ST2$^-$ Tregs (CD4$^+$CD25^{hi}ST2$^-$Foxp3$^+$). As expected, CD3/CD28–stimulated Th2 cells secreted significant levels of IL-10 and IL-13 (56, 57); however, the secretion of these cytokines was not modulated by IL-33, and thus was IL-33–independent (Figure 4, D and E, columns 7 and 8). Anti–CD3/CD28–stimulated or anti–CD3/CD28/IL-33–stimulated ST2$^-$ Tregs secreted very little IL-13 (Figure 4E, columns 1 and 3). They did secrete IL-10, but the quantity was much less than that produced by the other 3 CD4$^+$ T cell subsets (Figure 4D). CD4$^+$CD25^{lo}Foxp3$^+$ST2$^-$ T cells also exhibited this

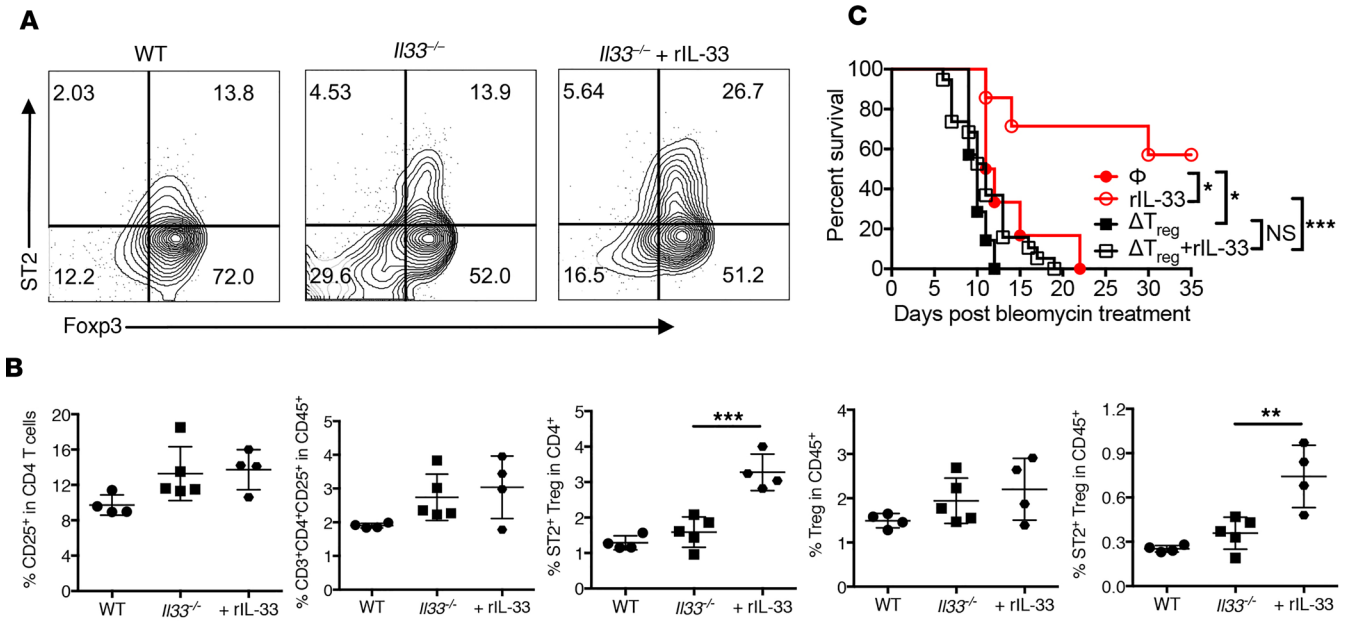

Figure 3. IL-33 increases Tregs that are required for protective functions of IL-33 after ALI. (**A** and **B**) Flow cytometric assessment of CD45$^+$CD3$^+$CD4$^+$CD25$^+$ cells isolated from enzymatically digested WT B6 and B6 *Il33*$^{-/-}$ mouse lung tissue at day 8 after bleomycin revealed that delivery of IL-33 increased ST2$^+$ Tregs in damaged *Il33*$^{-/-}$ lung tissue. Data depicted in **B** are the mean ± SD and are representative of 2 independent experiments, with 4–5 mice per group in each experiment. (**C**) Survival of B6 *Foxp3*^{DTR} mice injected i.t. with bleomycin alone or with rIL-33 (1 μg i.t.) in the presence of Tregs or following their deletion with diphtheria toxin (15 μg/kg on day −3, −2, and −1, and every other day starting from day 1). Depicted data represent 1 experiment with 6–7 mice per group. *P* values were determined by 1-way ANOVA followed by Tukey's multiple comparisons test (**B**) or log-rank test (**C**). **P* < 0.05; ***P* < 0.01; ****P* < 0.001. NS, not significant.

pattern of cytokine secretion (Figure 4, D and E, columns 5 and 6). ST2$^+$ Tregs were the most abundant producers of IL-10, but this production was IL-33–independent, as it was similar between anti–CD3/CD28– and anti–CD3/CD28/IL-33–stimulated groups (Figure 4D, columns 2 and 4). IL-33 stimulation of ST2$^+$ Tregs combined with anti–CD3/CD28 exposure did significantly increase their secretion of IL-13 (Figure 4E, columns 2 and 4). These data are consistent with recent findings from other groups and establish that ST2$^+$ Tregs secrete both IL-10, thought to support the suppressive capacity of Tregs (41), and IL-13, which has been suggested to result in a pathophysiologic role for Tregs during the development of allergic airway disease (43).

rIL-33 enhances expansion of suppressive IL-13–secreting human Tregs. We next determined whether rIL-33 facilitated these effects in human Tregs. We have established previously that the addition of rIL-33 to cultures of mouse monocyte-derived dendritic cells (Mono-DCs) and CD4$^+$ T cells was highly effective in expanding suppressive ST2$^+$ Tregs (54). As such, we relied on a modification of this approach to establish if IL-33 supported the expansion of human Tregs and to define whether IL-33 stimulation of human Tregs altered their suppressive capacity or production of IL-10 and IL-13. When rIL-33 was added to cultures of CD4$^+$CD25^{hi}CD127^{lo} Tregs flow-sorted from peripheral blood mononuclear cells (PBMCs) and allogeneic Mono-DCs, we observed that IL-33 did indeed support the expansion of human Tregs to a level that was comparable to what we had observed previously in mice (Figure 5A and Supplemental Figure 6A). During the 7-day culture, rIL-33–expanded Tregs maintained their suppressive function (Figure 5B). Furthermore, while IL-33 only slightly increased the secretion of IL-10 by human Tregs (Figure 5C), it profoundly increased their secretion of IL-13 (Figure 5D). We also verified that Tregs cultured with IL-33 expressed a high level of Foxp3 (Supplemental Figure 6B) and established that the IL-13 production was restricted to Foxp3^{hi} T cells (Figure 5E and Supplemental Figure 6C). In total, our data support the capacity of IL-33 to mediate the production of IL-13 by suppressive mouse and human Tregs.

Treg secretion of IL-13 is required to protect mice from mortality after ALI. To determine if IL-33–mediated local IL-13 secretion may have any protective function against ALI mortality we administered rIL-13 i.t. in conjunction with bleomycin challenge of *Il33*$^{-/-}$ mice and found that rIL-13 significantly improved their survival (Figure 6A). When we delivered rIL-13 with IL-33 to Treg-depleted *Foxp3*^{DTR} B6, we also found that rIL-13 significantly prolonged mouse survival after bleomycin injury (Figure 6B). These data suggest that IL-13 secreted by Tregs acts as a critical factor in the protective capacity of IL-33 after ALI.

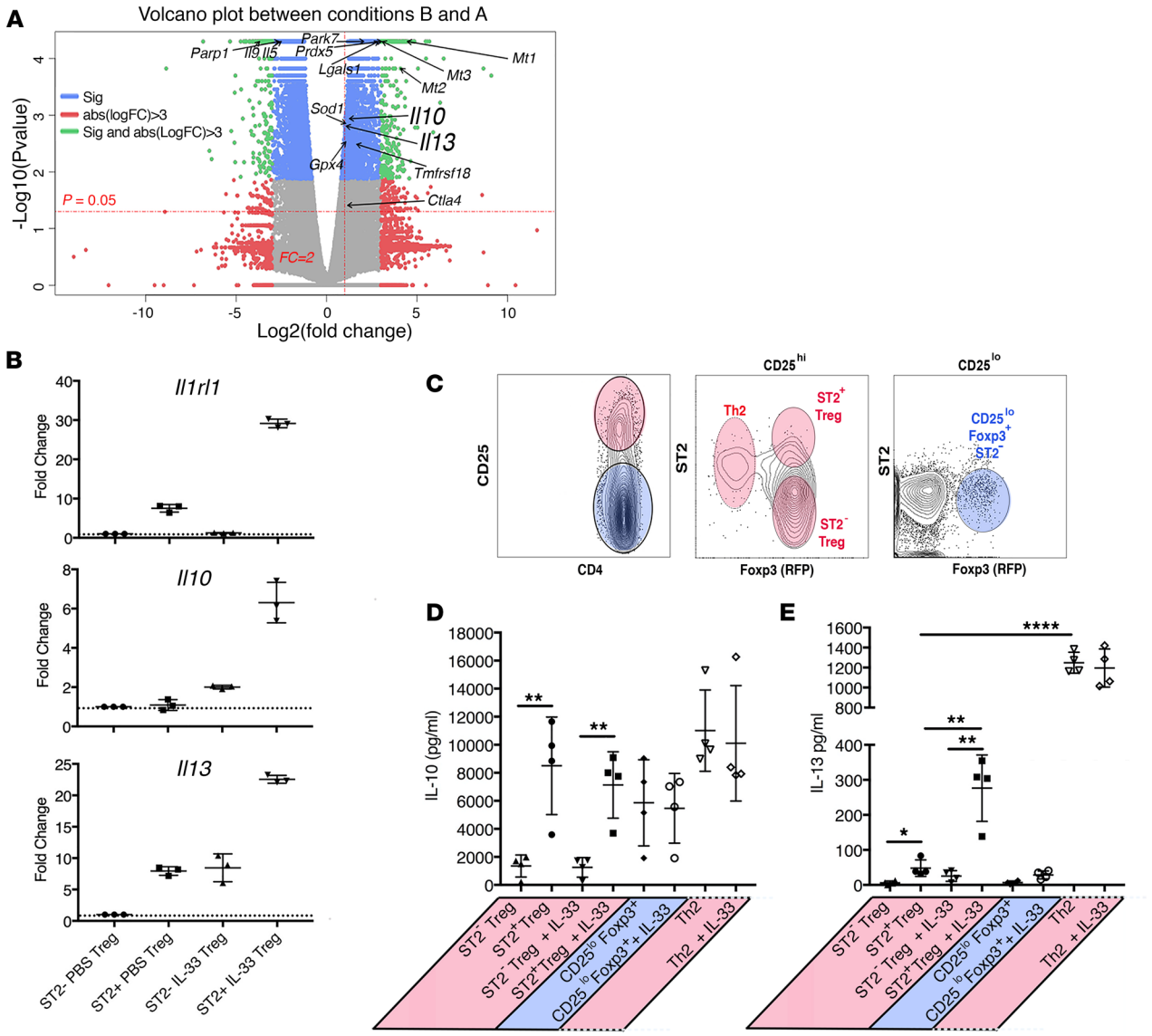

Figure 4. IL-33 stimulates the secretion of IL-13 by murine ST2⁺ Tregs. (**A**) Volcano plot depicting RNA-Seq analysis comparing ST2⁺ Tregs stimulated for 6 hours in the presence (condition B) or absence of IL-33 (20 ng/ml) (condition A) revealed increased transcripts for *Il10* and *Il13* after IL-33 stimulation. (**B**) qRT-PCR for *Il1rl1*, *Il10*, and *Il13* expressed by sorted CD4⁺Foxp3⁺ (RFP⁺) ST2⁻ or ST2⁺ cells from PBS- or IL-33–treated Foxp3-IRES-mRFP reporter mice confirmed RNA-Seq findings. Each column represents 3 mice. Data are from 1 experiment representative of 3 completed. (**C**–**E**) Representative flow cytometry plot (**C**) depicting the sorting strategy used for assessment of cytokine secretion by indicated CD4⁺ T cell populations after culture with or without IL-33 (20 ng/ml). Supernatants were harvested on day 3 of culture and assessed by Cytometric Bead Array (CBA) for (**D**) IL-10 and (**E**) IL-13. Statistical analysis with ANOVA was used to establish significance between values indicated. *$P < 0.05$; **$P < 0.01$; ****$P < 0.0001$.

To establish more precisely the role of Treg-secreted IL-13 in protection against ALI-induced mortality, we crossed Foxp3-IRES-Cre mice (58) to C.129P2(Cg)-*Il4/Il13*$^{tm1.1Lky}$/J (59) and demonstrated that sorted CD4⁺CD25⁺CD127^{lo} T cells from *Foxp3*^{Cre} × *Il4/Il13*$^{fl/fl}$ mice had substantially reduced IL-13 secretion relative to those from *Foxp3*^{Cre} littermates (Supplemental Figure 7, A and B). We observed residual IL-13 in *Foxp3*^{Cre} × *Il4/Il13*$^{fl/fl}$ CD4⁺CD25⁺CD127^{lo} T cell cultures (Supplemental Figure 7B) and we ascribe this to the presence of CD25^{hi}Foxp3⁻ Th2 cells that would have contaminated these cultures due to the lack of a *Foxp3*-driven reporter in this model to assist in their removal, as in Figure 4. While in theory, *Foxp3*^{Cre} × *Il4/Il13*$^{fl/fl}$ mouse T cells would also be deficient in IL-4, we have not observed that IL-33 induces any detectable Treg production of IL-4 in response to IL-33 (Supplemental Figure 8). Sorted *Foxp3*^{Cre} × *Il4/Il13*$^{fl/fl}$ CD4⁺CD25⁺CD127^{lo} cells displayed a suppressive capacity against anti–CD3/CD28–stimulated CD4⁺ and CD8⁺ T cells that was similar to IL-13–competent Tregs from *Foxp3*^{Cre} mice (Supplemental Figure 7C). Thus, the deletion of IL-13 from Tregs does not appear to alter their suppressive capacity.

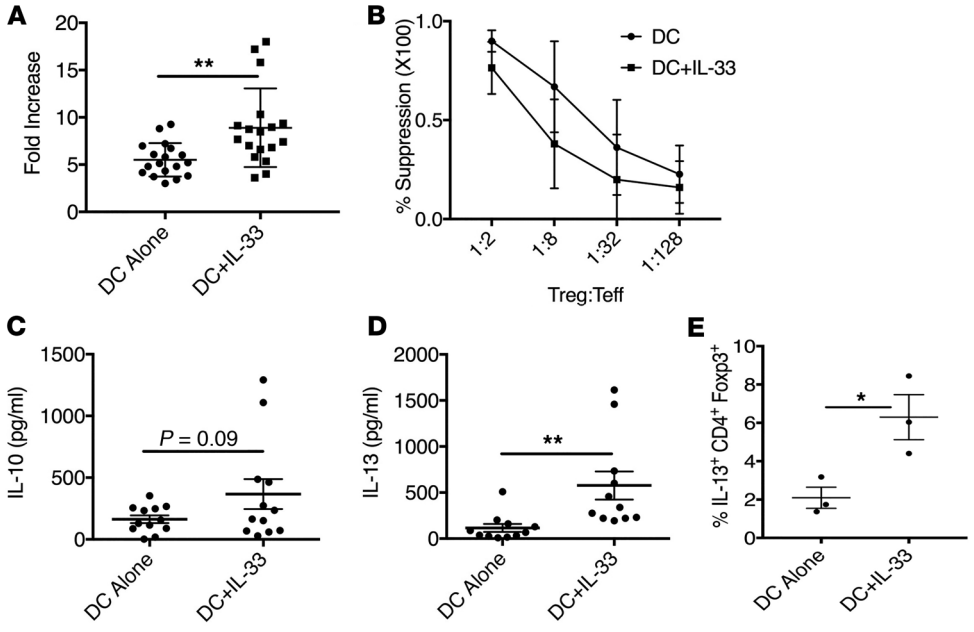

Figure 5. IL-33 expands suppressive human Tregs that secrete IL-13. (**A**–**D**) Human Tregs ($CD4^+CD25^{hi}CD127^{lo}$) sorted from peripheral blood mononuclear cells (PBMCs) were cultured with allogeneic monocyte-derived dendritic cells (Mono-DCs) and recombinant human IL-2 (300 U/ml) alone or with recombinant human IL-33 (50 ng/ml) added. (**A**) Cells were counted on the seventh day of culture and mean ± SD fold increase in Tregs depicted. Data represent 8 individual experiments with 18 different Treg and Mono-DC combinations. (**B**) Ex vivo–expanded Tregs from each culture condition were tested for their ability to suppress Teff proliferative responses to CD40L-activated allogeneic B cells. Treg suppressive function is expressed as percentage suppression of T cell proliferation and the mean ± SD from 5 cultures of expanded Tregs are depicted. (**C** and **D**) Supernatants were harvested on day 7 of culture and assessed by Cytometric Bead Array (CBA) for (**C**) IL-10 and (**D**) IL-13. Data depicted are the mean ± SD. (**E**) Mean frequency of IL-13+CD4+Foxp3^{hi} cells in cultures with and without IL-33 was determined by intracellular IL-13 and Foxp3 staining of one donor's Tregs following 7 days of culture with Mono-DCs generated from 2 different donors. Data depict Tregs from 3 different donors and are the mean ± SEM. Statistical significance was determined between each condition by unpaired, 2-tailed Student's *t* test. *$P < 0.01$, **$P < 0.01$.

When we examined how deletion of IL-13 from Tregs impacted bleomycin-induced ALI morbidity and mortality, we found that the phenotype of *Foxp3*^{Cre} × *Il4/Il13*$^{fl/fl}$ mice was very similar to that of *Il33*$^{-/-}$ mice. *Foxp3*^{Cre} × *Il4/Il13*$^{fl/fl}$ mice had significantly increased weight loss and exhibited reduced survival following bleomycin challenge compared with *Foxp3*^{Cre} controls (Figure 6, C and D). The dose of bleomycin was increased to 6.0 IU/kg in these studies to account for the BALB/c background of the *Foxp3*^{Cre} × *Il4/Il13*$^{fl/fl}$ and *Foxp3*^{Cre} mice and the appreciated resistance of BALB/c mice to bleomycin (60). These data indicate that Tregs are indeed an important source of protective IL-13 following chemically induced ALI. Completing an assessment of how IL-13 production by Tregs altered the local immune and cytokine environment early after bleomycin-induced lung injury revealed that, like the presence of IL-33, IL-13 produced by Tregs was a negative regulator of IL-6, G-CSF, and MCP-1/CCL2 at day 7 after bleomycin insult (Figure 6E). Comparison of the alveolar cellular infiltrates at day 7 after bleomycin between *Foxp3*^{Cre} × *Il4/Il13*$^{fl/fl}$ and *Foxp3*^{Cre} mice revealed that Treg deficiency of IL-13 did not appear to limit the decrease in frequency of AMs ($CD45^+CD11b^{lo}$Siglec-F^{hi}), but did result in an increase in the frequency of neutrophils ($CD45^+CD11b^{hi}$Siglec-F$^-$Ly6G^{hi}; Figure 6F and Supplemental Figure 9). Likewise, at day 7 after bleomycin, *Foxp3*^{Cre} × *Il4/Il13*$^{fl/fl}$ mice displayed increased frequency of inflammatory monocytes ($CD45^+CD11b^{hi}CD24^{lo}$MHC-II^{lo}Ly6C^{hi}; Figure 6F and Supplemental Figure 9).

To further assess the role of IL-13 secretion by Tregs in modulating local inflammation after virally induced ALI, *Foxp3*^{Cre} and *Foxp3*^{Cre} × *Il4/Il13*$^{fl/fl}$ mice received PR8 H1N1 influenza inoculation by oropharyngeal aspiration as we have described previously (61). The findings in these studies were highly reflective of those observed following bleomycin administration. Once again, *Foxp3*^{Cre} × *Il4/Il13*$^{fl/fl}$ mice displayed significantly increased weight loss compared with *Foxp3*^{Cre} controls (Supplemental Figure 10A), which was not due to altered viral clearance (Supplemental Figure 10B). Although we did not observe differences in

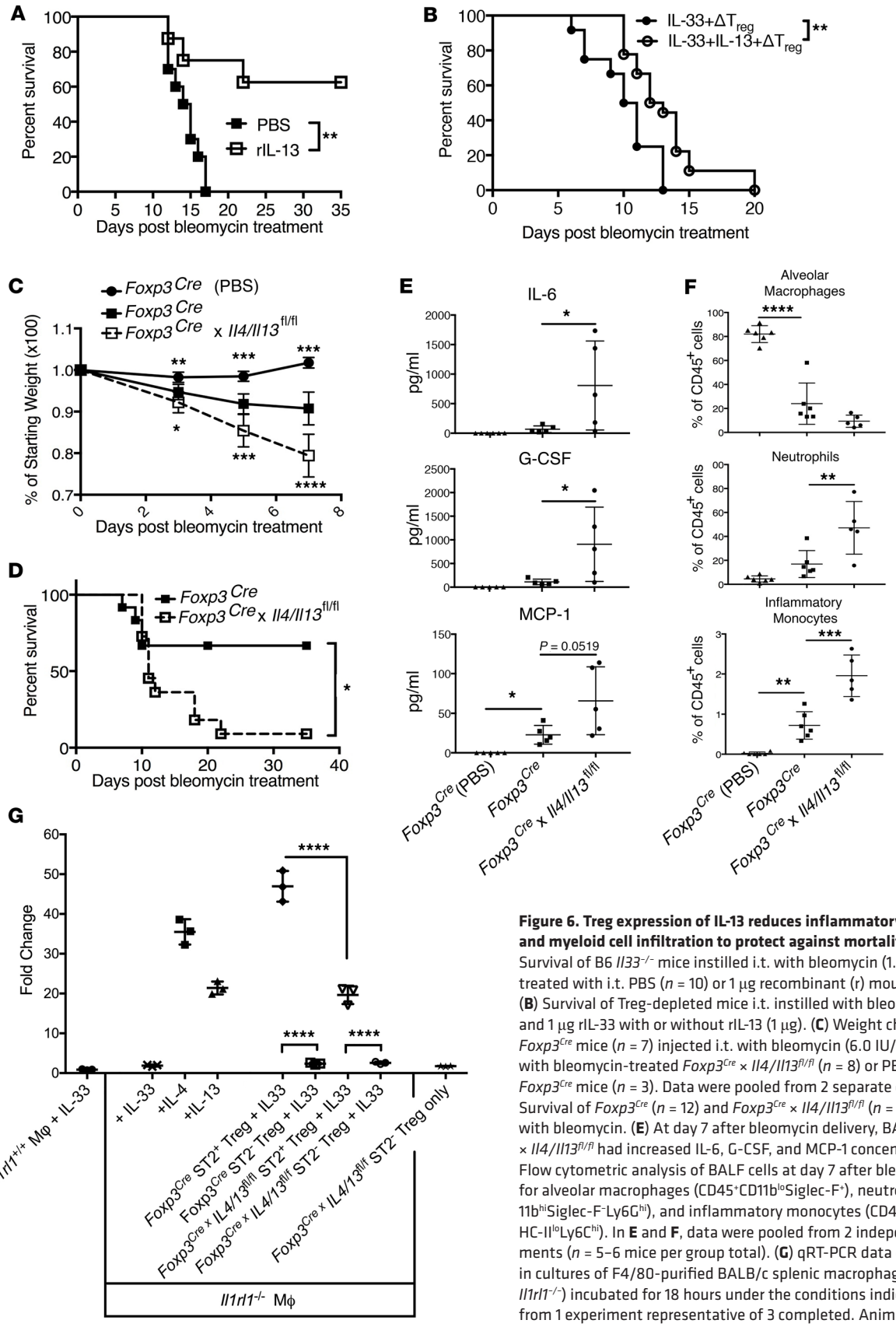

Figure 6. Treg expression of IL-13 reduces inflammatory cytokines and myeloid cell infiltration to protect against mortality after ALI. (**A**) Survival of B6 *Il33*$^{-/-}$ mice instilled i.t. with bleomycin (1.0 IU/kg) and also treated with i.t. PBS (n = 10) or 1 μg recombinant (r) mouse IL-13 (n = 8). (**B**) Survival of Treg-depleted mice i.t. instilled with bleomycin (1.0 IU/kg) and 1 μg rIL-33 with or without rIL-13 (1 μg). (**C**) Weight changes of BALB/c *Foxp3*^{Cre} mice (n = 7) injected i.t. with bleomycin (6.0 IU/kg) compared with bleomycin-treated *Foxp3*^{Cre} × *Il4/Il13*$^{fl/fl}$ (n = 8) or PBS-treated *Foxp3*^{Cre} mice (n = 3). Data were pooled from 2 separate experiments. (**D**) Survival of *Foxp3*^{Cre} (n = 12) and *Foxp3*^{Cre} × *Il4/Il13*$^{fl/fl}$ (n = 11) injected i.t. with bleomycin. (**E**) At day 7 after bleomycin delivery, BALF from *Foxp3*^{Cre} × *Il4/Il13*$^{fl/fl}$ had increased IL-6, G-CSF, and MCP-1 concentrations. (**F**) Flow cytometric analysis of BALF cells at day 7 after bleomycin delivery for alveolar macrophages (CD45^{+}CD11b^{lo}Siglec-F^{+}), neutrophils (CD45^{+}CD11b^{hi}Siglec-F^{-}Ly6G^{hi}), and inflammatory monocytes (CD45^{+}CD11b^{hi}CD24^{lo}MHC-II^{lo}Ly6C^{hi}). In **E** and **F**, data were pooled from 2 independent experiments (n = 5–6 mice per group total). (**G**) qRT-PCR data of *Arg1* expression in cultures of F4/80-purified BALB/c splenic macrophages (*Il1rl1*$^{+/+}$ or *Il1rl1*$^{-/-}$) incubated for 18 hours under the conditions indicated. Data are from 1 experiment representative of 3 completed. Animal survival was compared by Kaplan-Meier analysis and the log-rank test. Data are the mean ± SD and P values were determined by 2-tailed Student's t test or 1-way ANOVA. *P < 0.05; **P < 0.01; ***P < 0.001; ****P < 0.0001.

BALF levels of IgM or total protein (Supplemental Figure 10C), *Foxp3*^{Cre} × *Il4/Il13*$^{fl/fl}$ mice also again had an increased frequency of inflammatory monocytes at day 7 after infection (Supplemental Figure 10D). In total, our data generated using this mutant-Treg mouse in 2 distinct models of ALI support a critical role for IL-13 secreted by Tregs for regulation of the early inflammatory response, especially the accumulation of neutrophils and inflammatory monocytes after lung injury.

Arginase 1 (*Arg1*) is commonly expressed by immunoregulatory or reparative myeloid cells (62–64). Interestingly, we could show that while rIL-33 alone did not induce *Arg1* expression in either *Il1rl1*$^{-/-}$ or *Il1rl1*$^{+/+}$ splenic macrophages ex vivo (Figure 6G, columns 1 and 2), IL-33–stimulated ST2$^+$ Tregs did effectively induce Arg1 in *Il1rl1*$^{-/-}$ splenic macrophages (Figure 6G, column 5). These data suggest that ST2$^+$ Tregs can be stimulated by IL-33 to support the differentiation of myeloid cells towards that of those with reparative or regulatory functions, such as myeloid-derived suppressor cells (MDSCs) or reparative macrophages (62–64). This capacity was reduced significantly when IL-13 was deleted from Foxp3-expressing cells (Figure 6G, column 7). These data suggest that IL-33–mediated Treg secretion of IL-13, while not important for suppressive function, may act as a potent modulator of infiltrating myeloid cells after tissue injury.

Discussion

We have made several impactful findings in the current studies. First, by demonstrating the sensitivity of IL-33–deficient mice to bleomycin-induced ALI and the reversibility of this phenotype by complementation with rIL-33, we have established that IL-33 is a crucial local factor necessary to limit the early inflammatory response after chemically induced ALI. Second, we found that Tregs are the cellular mediator of the protective capacity of IL-33 after ALI. Third, we demonstrated that IL-33–stimulated IL-13 production by Tregs is critical for controlling inflammation after chemically and virally induced ALI and can shape macrophage activation ex vivo.

Our observations may seem counterintuitive, given the compelling evidence for a pathological role for IL-13 in tissue fibrosis and asthma development (65–68). Yet, IL-13 has also become known for regenerative and reparative functions, due in large part to its capacity to activate tissue-repair macrophages (62, 69–71). Recently, it was demonstrated that ILC2-produced IL-13 promotes lung regeneration after pneumonectomy by stimulating macrophage support of type 2 alveolar epithelial stem cell proliferation (72). GVHD studies demonstrate potent protective capacities of ILC2-secreted IL-13, which diminished Th1 and Th17 responses, generated MDSCs, aided gastrointestinal homeostasis, and promoted animal survival (73). IL-13 administration to GM-CSF– and G-CSF–driven bone marrow cultures generates Arg1$^+$ MDSCs able to limit GVHD lethality through immune regulation (74). Our current study establishes that in the absence of IL-13 expression by Tregs, ALI results in increased lethality associated with augmented frequency of phenotypic inflammatory monocytes. We also find that IL-33–stimulated Tregs secreting IL-13 directly induce *Arg1* gene expression in splenic macrophages. These data are similar to recent ex vivo studies demonstrating that Treg-produced IL-13 stimulates IL-10 production in interacting macrophages to support macrophage efferocytosis of apoptotic cells (75). Together, our studies define an important role for IL-33 stimulation of Treg secretion of IL-13 for control of the myeloid response and inflammation after injury.

Peripheral tissues, including the lung, have higher frequencies of ST2$^+$ Tregs relative to the secondary lymphoid organs (SLOs) (Supplemental Figure 3C and refs. 42, 55, 76). Yet, due to the greater overall immune cell number of the spleen, the incidence of ST2$^+$ Tregs in the spleen is comparatively quite high relative to the lung. Importantly, unlike macrophages, there is no existing evidence suggesting that Tregs within peripheral tissues are embryonically distinct from those of SLOs (77, 78). Therefore, we chose to compare splenic ST2$^+$ versus ST2$^-$ Tregs in the mechanistic and characterization studies requiring high cell numbers. Consistent with our previous findings (54) and those of others (55, 79), ST2$^+$ Tregs from both lymphoid and nonlymphoid tissues showed higher expression of activation markers including CD44, CD103, and killer cell lectin-like receptor subfamily G member 1 (KLRG1), and suppressor functional molecules such as OX40 and glucocorticoid-induced TNFR-related protein (GITR), compared with ST2$^-$ Tregs (Supplemental Figure 3D). These data suggest that ST2$^+$ Tregs are a comparable population, regardless if they are isolated from SLOs or nonlymphoid peripheral tissue. A recent comparison of the DNA methylome and transcriptome of ST2$^+$ and ST2$^-$ Tregs from nonlymphoid peripheral tissue and SLOs supports the conclusion that ST2$^+$ Tregs in the spleen have transcriptomic and epigenomic patterns highly comparable to peripheral tissue ST2$^+$ Tregs and that splenic ST2$^+$ Tregs represent a recirculating fraction of tissue-resident Tregs (55). For these reasons, we are confident in extrapolating findings based on the mechanistic study of splenic Tregs to tissue Tregs in the lung.

While our ex vivo data using splenic macrophages suggest that Treg-produced IL-13 can act directly on infiltrating myeloid cells to induce gene expression representative of reparative or regulatory myeloid activity, lung epithelial cells can also express IL-13 receptors (IL-13Rs) (80), and both myeloid and epithelial cells can release IL-6, MCP-1/CCL2, and G-CSF (81–83), which we found increased in the BALF in the absence of IL-33 or Treg IL-13. By using WT or *Il13ra1*$^{-/-}$ bone marrow–chimeric mice, Karo-Atar et al. suggested that IL-13R in both hematopoietic and structural cells (epithelial cells and fibroblasts) played a role in tissue repair after bleomycin-induced lung injury (84). These findings are consistent with ours in their support for a critical role of IL-13 signaling in protection after ALI. However, the chimeric animal models used by Karo-Atar et al. were unable to delineate the cell type that was instrumental in IL-13–mediated protection after injury, as they resulted in both hematopoietic and nonhematopoietic cell engraftment. A prior study has also demonstrated that rIL-4 administration after LPS-induced ALI resulted in increased survival and improved lung function (85). In this study, the authors demonstrated that this effect was due to an IL-4–mediated, STAT6-dependent reprogramming of macrophages towards antiinflammatory subsets and did not require Tregs. While we do not find that IL-33 induces IL-4 production by Tregs (Supplemental Figure 8), our current findings are compatible with this study, as IL-13 produced by Tregs would activate this same STAT6-dependent pathway in local myeloid cells and stromal cells. Furthermore, several reports have suggested an important reparative relationship between IL-33 and Treg production of amphiregulin (AREG) after injury of the lung, muscle, and brain (40, 42, 86). In the current study, we have now identified a mechanism by which IL-33–stimulated Tregs support inflammation resolution through secretion of IL-13. Moving forward, it will be important to determine if IL-33–stimulated Treg expression of IL-13 supports resolution of early inflammation by targeting resident AMs and infiltrating myeloid cells, altering stromal cell cytokine and chemokine expression, or both. Likewise, establishing how Tregs use secretion of reparative molecules such as AREG, myeloid-shaping factors like IL-13 and IL-10, and T cell–suppressive functions to control inflammation and resolve wounds is important basic knowledge and would be broadly impactful. This knowledge may allow development of therapies designed to augment required Treg functions or lead to novel cell therapies utilizing Tregs generated specifically to perform repair, suppress myeloid cell inflammation, or control T effectors.

After alveolar barrier disruption, dysregulated inflammation and immune cell activity can lead to increased ALI pathology and ARDS (1, 2). Failure to rapidly resolve inflammation and associated tissue injury, support alveolar progenitor cell renewal, and direct appropriate regeneration of the alveolar epithelium can also lead to pulmonary fibrosis (87). IL-33 is constitutively expressed, but sequestered, in the lung epithelium and type 2 alveolar cells (AEC2s) of both mice and humans (88–91). Upon its release due to local injury or following systemic trauma, IL-33 appears to play a complex, yet integral role in shaping early inflammation, resolution of inflammation and injury, as well as fibrotic disease development in the lung. Numerous immune cells express ST2 constitutively or can be induced to express it (35). We have recently established that IL-33 is detectable in the serum of rodents and patients 6 to 12 hours after blunt trauma, and targeted ST2^{+} ILC2s and cause early lung injury mediated by ILC2-secreted IL-5 and CXCR2^{+} lung neutrophils (92). Yet, these current studies would suggest that early inflammatory functions of IL-33 may rapidly give way to IL-33–triggered protective mechanisms involving Tregs. Our data demonstrating a protective role for IL-13 are similar to the recent observation that IL-5 produced by ICOS^{+} ILC2s can support survival after bleomycin-induced ALI (93). Yet, it is easy to envision how sustained or repeated release of IL-33, even if targeting ST2^{+} Tregs to secrete IL-13 or ILC2 release of IL-5, could eventually transition to a detrimental role and support fibrotic disease or general inflammatory processes (45, 94).

Furthermore, we found that both IL-33 and IL-13 secretion by Tregs modulated IL-6, G-CSF, and MCP-1/CCL2 after bleomycin-induced ALI. This is consistent with prior studies where CD4^{+}CD25^{+} T cells were demonstrated to suppress IL-6 and MCP-1/CCL2 after LPS-mediated ALI (29). While it is tempting to conclude that a reduction of these effector molecules underlies the observed decrease in mortality after ALI, like IL-33 and IL-13, these molecules possess a pleiotropic nature during ALI. IL-6 is a mediator of acute-phase inflammation and orchestrates the immune responses leading to fibrosis after bleomycin insult (95, 96), but IL-6 is also important for supporting alveolar progenitor renewal (97, 98). Blocking G-CSF signaling reduces inflammation and MCP-1/CCL2 levels (99). Monocyte recruitment to the inflamed lung is dependent on CCR2 and serves to accelerate and augment neutrophil accumulation (100, 101). Intraperitoneal bleomycin delivery to *Ccl2*$^{-/-}$ mice fails to instigate the typical monocytic lung inflammation or cause significant lung fibrosis (102). Sustained expression of MCP-1/CCL2 is associated

with increased recruited macrophages in ARDS patients and worse prognosis (6, 103). Thus, the local regulation of MCP-1/CCL2 by ST2$^+$ Tregs stimulated with released IL-33 could be an important mechanism to control pathology early after ALI. However, mice with lung-specific overexpression of MCP-1/CCL2 display resistance to bleomycin-induced lung injury (104). This was due to an increased ability of MCP-1/CCL2-overexpressing mice to recruit a monocyte/macrophage subpopulation that mediates clearance of apoptotic neutrophils. As such, these mice could better complete a critical step in the initiation of inflammation resolution after ALI (2). The complexity of the cytokine and immune cell networks that control an interrelated inflammatory and resolution/repair response are quite evident. It is safe to conclude that IL-33 is as an important tissue-derived signaling molecule that is active in both the inflammatory and resolution/repair phases after tissue injury. Our current studies place IL-33 upstream of a potent Treg response that dampens early inflammatory responses after injury and is required to survive an insult to the lung epithelium. It will now be important to use techniques such as bioinformatics and mathematical modeling of the immune cell/cytokine interactions (92) to establish how these pleiotropic cytokines, chemokines, and alarmins interact with a changing collection of localized immune cells at each step after injury, inflammation, resolution, and remodeling. Such studies will provide a framework to develop precision-medicine approaches where biologicals targeting specific cells or cytokines/chemokines are delivered after first determining what cytokine/immune networks are dominant. This approach would allow care providers to orchestrate the appropriate immunological or physiological outcome.

Patients that develop ARDS have long suffered significant morbidity and mortality (105). A recent study involving intensive care units (ICUs) from 50 countries demonstrated that 10.4% of ICU patients and 23.4% of mechanically ventilated patients suffered ARDS, of which mortality ranged from 34.9% to 46.1% (4). Despite intensive basic and clinical research, there are few effective targeted ARDS therapies apart from mechanical ventilation (8, 18). Consequently, there remains a need for understanding the pathophysiology underlying ARDS and ALI to identify molecular targets for the development of effective therapies. In the current studies, we identify endogenous IL-33 and Treg-secreted IL-13 as critical molecules that are essential to control the early inflammatory response after or during ALI. Our mechanistic studies reveal that the effect of IL-33 and IL-13 in limiting local inflammatory responses may be mediated, at least partially, by shaping the myeloid compartment after lung injury. Our findings provide a pathway to develop immunotherapies that could improve clinical outcome of ALI/ARDS. Remarkably, we showed a potent effect of a single dose of exogenous rIL-33 or rIL-13 in decreasing lethality after bleomycin-induced ALI. This is very clinically relevant and exploration of the IL-33/Treg pathway in clinical ALI and ARDS warrants further exploration.

Methods

Mouse strains. C57BL/6-*Foxp3*^{tm1Flv}/J (Foxp3-IRES-mRFP, referred to as "B6 FIR"), B6.129(Cg)*Foxp3*$^{tm3(DTR/GFP)Ayr}$/J (Foxp3-DTR-EGFP), and C.129P2(Cg)-*Il4/Il13*$^{tm1.1Lky}$/J (BALB/c *Il4/Il13*^{flox}) mice were purchased from The Jackson Laboratory. C57BL/6NTac mice were obtained from Taconic. B6 *Il33*$^{-/-}$ have been previously described (106) and were obtained from RIKEN (account CDB0631K, http://www2.clst.riken.jp/arg/TG%20mutant%20mice%20list.html). *Foxp3*-IRES-Cre mice (BALB/c *Foxp3*^{Cre}; ref. 58) were obtained from Dario Vignali (University of Pittsburgh). Previously described BALB/c *Il1rl1*$^{-/-}$ were obtained from Foo Yew Liew (University of Glasgow) (51, 107). All mice were bred and/or maintained in a specific pathogen–free animal facility at the University of Pittsburgh.

Animal treatments. For chemically induced ALI, mice were i.t. instilled with 1.0–1.5 IU/kg (for mice on B6 background) or 6.0 IU/kg (for BALB/c background) bleomycin (APP Pharmaceuticals, LLC) on day 0. Mouse rIL-33 (1.0 μg/mouse; Biolegend) was instilled i.t. 1 time together with bleomycin on day 0. For rIL-13 administration (1.0 μg/mouse; Biolegend), the first dose was i.t. injected together with bleomycin on day 0 and later doses rIL-13 were instilled intranasally (i.n.) on day +1, +2, and +3. For Treg depletion, *Foxp3*^{DTR} mice were treated with 15 μg/kg DT (Sigma-Aldrich) on day –3, –2, and –1, and every other day starting from day 1. For virally induced ALI, influenza A PR/8/34 H1N1 was used to inoculate mice with 100 plaque-forming units of influenza in 50 μl of sterile PBS by oropharyngeal aspiration on day 0. Viral burden was determined by qRT-PCR on lung RNA for viral matrix as previously described (61). The weight and survival of treated animals was monitored. In survival studies, survival was defined as death or euthanasia after sustained weight loss greater than 30%–35% of the starting weight. See supplemental methods for detailed descriptions of the lung inflammation assessment and histopathological evaluations completed after ALI.

Culture of human Mono-DCs and Tregs. $CD4^+CD127^{lo}CD25^{hi}$ Tregs were isolated by FACS with a BD FACSAria following isolation of Pan T cells by negative selection from $CD14^-$ PBMCs using a human Pan T cell isolation kit (Miltenyi Biotec). Mono-DCs were suspended in OpTmizer (ThermoFisher Scientific) supplemented with 5% human AB serum, irradiated at 30 Gy and plated in 48-well plates at a ratio of 4 Tregs to 1 Mono-DC. Human rIL-2 (300 U/ml; Peprotech) alone or with human rIL-33 (50 ng/ml; R&D Systems) was added on day 2. On day 4, half of the medium was exchanged and cytokines refreshed. On day 7, Tregs were analyzed for Foxp3 and IL-13 expression by flow cytometry, suppressive capacity assessed, or transferred to new plates and further expanded in OpTmizer and cytokines until day 12.

Flow cytometry. Alveolar leukocytes were obtained by centrifugation of BALF collected using methods similar to those described previously (104, 108). To assess interstitial leukocytes, mouse lungs were cut into small pieces and enzymatically digested using either collagenase D and DNase I (both from Sigma-Aldrich) or a lung dissociation kit (Miltenyi Biotec) followed by mechanical dissociation in C tubes using a gentleMACS dissociator (Miltenyi Biotec). Single-cell homogenates of splenocytes were generated for flow cytometric assessment using standard and widely published laboratory procedures. Isolated cells were incubated with anti-CD16/32 (clone 93, for FcR block) and Zombie NIR (for cell viability, both from Biolegend) before staining with the following antibodies: anti-CD45 (clone 30-F11), -CD3e (clone 145-2C11), -CD4 (clone RM4-5), -CD25 (clone PC61), -CD11b (clone M1/70), -CD11c (clone HL3), –Ly-6C (clone AL-21), –Ly-6G (clone 1A8), –Siglec-F (clone E50-2440), –I-A/I-E (clone 2G9), -CD24 (clone M1/69), -CD44 (clone IM7), -CD86 (clone GL-1), -CD103 (clone M290), -CD19 (clone 1D3), –Sca-1 (clone D7), -NK1.1 (clone PK136), -Gr1 (clone RB6-8C5), -CD127 (clone SB/199), -ICOS (clone C398.4A), -OX40 (clone OX-86), -GITR (clone DTA-1), -KLRG1 (clone 2F1, all from BD Biosciences); and anti-ST2 (clone DJ8, MD Biosciences). For ILC2 staining, lineage markers included CD3, CD4, CD8, CD19, B220, CD11b, CD11c, FcεRI, GR1, NK1.1, and TER119. For intracellular Foxp3 staining, Intracellular Fixation & Permeabilization buffer set and anti-Foxp3 (clone FJK-16s, both from eBioscience) were used per the manufacturer's instructions. Cultured human Tregs were restimulated for 3 hours with phorbol 12- myristate-13-acetate with GolgiPlug (BD Biosciences), and then surface stained with BD Bioscience antibodies against CD3 (clone UCHT1) and CD4 (clone RPA-TF), and then subsequently stained for intracellular IL-13 (clone JES10-5A2) and Foxp3 (clone 259D/C7). All samples were acquired with an LSRFortessa or LSRII (BD Biosciences) and data were analyzed with FlowJo (BD Biosciences).

RNA-Seq and bioinformatics analyses. Splenic $CD4^+$ T cells were obtained from B6 FIR mice using negative depletion with Dynabeads (Life Technologies) as we have previously described in detail (51). These cells were cultured for 5 days with BALB/c $CD11c^+$ bone marrow–derived DCs generated as we have previously described (54) in media supplemented with rIL-33 (20 ng/ml; Biolegend). Cultured cells were then stained with antibodies against CD4 and ST2, and the $CD4^+Foxp3^+$ (RFP^+) $ST2^+$ population flow sorted to greater than 95% purity using a BD FACSAria. Sorted cells were rested for 15–18 hours in complete RPMI at 5% CO_2 and 37°C, followed by a 6-hour period in which they remained untreated or were stimulated with 100 ng/ml mouse rIL-33 during the culture period. Cells were collected and RNA extracted after lysing in TRIzol reagent (ThermoFisher Scientific) according to manufacturer's instructions. RNA-Seq analysis was completed by the University of Pittsburgh Health Sciences Core Research Facilities (HSCRF) shared Genomics Research Core. Detailed description of the RNA-Seq methods and analysis are provided in the supplemental methods. The RNA-Seq data have been deposited in the NCBI's Gene Expression Omnibus (GEO) and are accessible as GSE123922.

qRT-PCR on splenic Tregs for Il1rl1, Il10, and Il13 mRNA. B6 FIR mice were treated for 10 days with rIL-33 in PBS (1 μg/mouse/day, Biolegend) or treated with PBS alone. On day 11, $CD4^+$ T cells were sorted by FACS into $ST2^-$ and $ST2^+$ $Foxp3^+$ (RFP^+) populations, which were used to generate total RNA that was assessed by qRT-PCR for *Il1rl1*, *Il10*, and *Il13* mRNA. See supplemental methods for detailed descriptions of qRT-PCR methodology.

Treg suppression assays. For mouse assays, bulk $CD4^+$ T cells were negatively selected from BALB/c *Foxp3*^{Cre} BALB/c and *Foxp3*^{Cre}*Il4/13*$^{fl/fl}$ spleens using Dynabeads and stained for FACS (FACSAria) of $CD3^+CD4^+CD127^{lo}CD25^{hi}$ Tregs. Sorted Tregs were tested for their ability to suppress anti–CD3/CD28 T-activator bead–induced (5×10^4; Life Technologies), CellTrace Violet Blue–labeled (BD Biosciences) BALB/c $CD3^+$ T cell (T effector [Teff]) proliferation at Teff/Treg ratios of 8:1, 4:1, and 2:1. Cells were harvested on day 3 and stained intracellularly for FACS analysis. For assessment of human Treg suppressive capacity, cryopreserved Teffs, ex vivo–expanded Tregs, and CD40L-activated allogeneic B cells were counted before

the Teffs were labeled with V450 Proliferation Dye (BD Biosciences) and Tregs and B cells labeled with carboxyfluorescein succinimidyl ester (BD Biosciences). Labeled cells were suspended in RPMI at 2×10^6/ml for Teffs, 5×10^5/ml for Tregs, and 5×10^5/ml for B cells. Tregs were diluted from 1:2 to 1:128 relative to Teffs, while B cell numbers were held constant. Cells were cultured for 5 days before analysis for proliferation was assessed by flow cytometry.

CBA assessment of Treg cytokine secretion. B6 FIR, BALB/c *Foxp3*^{Cre}, and *Foxp3*^{Cre}*Il4/13*$^{fl/fl}$ mice were either treated for 10 days with mouse rIL-33 in PBS (1 μg/mouse/day, Biolegend) or remained PBS treated. On day 11, CD3$^+$CD4$^+$CD127^{lo}CD25^{hi} ST2$^+$ and ST2$^-$ Tregs were FACS isolated and plated in flat-bottom 96-well plates coated with anti-CD3 (Bio X Cell, 5 μg/ml) in RPMI containing 10% FBS, 2 mM L-glutamine, 0.05 mM 2-mercaptoethanol, 1× MEM Non-Essential Amino Acids, 10 mM HEPES, 1 mM sodium pyruvate, and 100 U/ml each of penicillin and streptomycin. Anti-CD28 (BD Biosciences, 2 μg/ml) and human rIL-2 (Peprotech, 50 U/ml) were added for T cell activation. Some wells were treated with 20 ng/ml mouse rIL-33. After 3 days, the culture supernatants were harvested and analyzed by Cytometric Bead Array (CBA; BD Biosciences) per the manufacturer's instruction for mouse IL-4, IL-13, and IL-10. To measure human Treg cytokine secretion, cell-free supernatants were collected on day 7 of Mono-DC and Treg culture and analyzed for IL-10 and IL-13 by CBA. Data were collected using a BD LSRFortessa cytometer and analyzed using FCAP Array software (BD).

qRT-PCR for myeloid skewing by Tregs. BALB/c *Foxp3*^{Cre} and *Foxp3*^{Cre}*Il4/13*$^{fl/f}$ mice were treated for 10 days with 0.5 μg/mouse/day rIL-33. On day 11, splenocytes were harvested and CD3$^+$CD4$^+$CD127^{lo}CD25^{hi} ST2$^+$ and ST2$^-$ Tregs isolated by FACS. On the same day, splenic macrophages from *Il1rl1*$^{+/+}$ and *Il1rl1*$^{-/-}$ mice were isolated by magnetic positive selection using F4/80 beads (Miltenyi Biotec). Tregs and macrophages were cocultured and treated with 20 ng/ml rIL-4, 200 ng/ml mouse rIL-13 (Biolegend), or 20 ng/ml mouse rIL-33 (Biolegend). After 18 hours, the cells were harvested and isolated total RNA assessed for *Arg1* and *18s* mRNA. See supplemental methods for more details.

Statistics. GraphPad Prism was used for statistical analyses. Results are presented as means ± SD. Statistical significance was determined by unpaired 2-tailed Student's *t* test, Mann-Whitney test, 1-way ANOVA followed by Tukey-Kramer multiple comparisons test, or log-rank (Mantel-Cox) test. In all cases, a P value < 0.05 was considered statistically significant. Outliers were identified using the ROUT method and a Q value of 1%.

Study approval. All rodent breeding and experimental procedures were approved by and performed in accordance with the guidelines of the Institutional Animal Care and Use Committee of the University of Pittsburgh and complied with the NIH *Guide for the Care and Use of Laboratory Animals* (National Academies Press, 2011). Normal human blood products were obtained and utilized in accordance with University of Pittsburgh Institutional Review Board procedures.

Author contributions

QL, GKD, AWT, JFA, KMR, MHF, TRB, and HRT conceptualized and designed the research. QL, GKD, YZ, HL, LRM, KMR, MHF, and HRT performed the experiments. QL, GKD, YZ, HL, LRM, ABC, URC, JAD, LAO, BRP, AWT, KMR, MHF, and HRT analyzed the data and interpreted the results of the experiments. QL, GKD, and HRT prepared the figures. QL, GKD, LAO, JFA, BRP, AWT, TRB, and HRT drafted and edited the manuscript.

Acknowledgments

We acknowledge the excellent manuscript preparation support of Carla Forsythe. We thank Anna Lucas for her technical assistance. This work was supported by NIH grants R01HL122489 and R21AI121981 (to HRT) and R01AI18777 and U19AI131453 (to AWT). GKD was supported by NIH grant T32CA082084. This project utilized the University of Pittsburgh HSCRF Genomics Research Core for RNA-Seq services. Luminex assays were completed by the UPCI Cancer Biomarkers Facility: Luminex Core Laboratory that is supported in part by award P30CA047904. This work also benefitted from the use of a BD LSRFortessa obtained with funding from the NIH (1S10OD011925-01).

Address correspondence to: Timothy R. Billiar, F1281 Presbyterian University Hospital, 200 Lothrop Street, University of Pittsburgh Department of Surgery, Pittsburgh, Pennsylvania 15261, USA. Phone: 412.647.1749; E-mail: billiartr@upmc.edu. Or to: Hēth R. Turnquist, E1554 Biomedical Science Tower, 200 Lothrop Street, Pittsburgh, Pennsylvania 15261, USA. Phone: 412.624.6695; E-mail: Het5@pitt.edu.

1. Ware LB, Matthay MA. The acute respiratory distress syndrome. *N Engl J Med*. 2000;342(18):1334–1349.
2. Matthay MA, Ware LB, Zimmerman GA. The acute respiratory distress syndrome. *J Clin Invest*. 2012;122(8):2731–2740.
3. Wheeler AP, Bernard GR. Acute lung injury and the acute respiratory distress syndrome: a clinical review. *Lancet*. 2007;369(9572):1553–1564.
4. Bellani G, et al. Epidemiology, patterns of care, and mortality for patients with acute respiratory distress syndrome in intensive care units in 50 countries. *JAMA*. 2016;315(8):788–800.
5. Bauer TT, et al. Comparison of systemic cytokine levels in patients with acute respiratory distress syndrome, severe pneumonia, and controls. *Thorax*. 2000;55(1):46–52.
6. Aggarwal NR, King LS, D'Alessio FR. Diverse macrophage populations mediate acute lung inflammation and resolution. *Am J Physiol Lung Cell Mol Physiol*. 2014;306(8):L709–L725.
7. Zemans RL, Matthay MA. What drives neutrophils to the alveoli in ARDS? *Thorax*. 2017;72(1):1–3.
8. Thompson BT, Chambers RC, Liu KD. Acute respiratory distress syndrome. *N Engl J Med*. 2017;377(19):1904–1905.
9. McAuley DF, et al. Simvastatin in the acute respiratory distress syndrome. *N Engl J Med*. 2014;371(18):1695–1703.
10. National Heart, Lung, Blood Institute ARDS Clinical Trials Network, et al. Rosuvastatin for sepsis-associated acute respiratory distress syndrome. *N Engl J Med*. 2014;370(23):2191–2200.
11. Ferguson ND, et al. High-frequency oscillation in early acute respiratory distress syndrome. *N Engl J Med*. 2013;368(9):795–805.
12. Young D, et al. High-frequency oscillation for acute respiratory distress syndrome. *N Engl J Med*. 2013;368(9):806–813.
13. Spragg RG, et al. Effect of recombinant surfactant protein C-based surfactant on the acute respiratory distress syndrome. *N Engl J Med*. 2004;351(9):884–892.
14. Paine R, et al. A randomized trial of recombinant human granulocyte-macrophage colony stimulating factor for patients with acute lung injury. *Crit Care Med*. 2012;40(1):90–97.
15. Steinberg KP, et al. Efficacy and safety of corticosteroids for persistent acute respiratory distress syndrome. *N Engl J Med*. 2006;354(16):1671–1684.
16. Bernard GR, et al. High-dose corticosteroids in patients with the adult respiratory distress syndrome. *N Engl J Med*. 1987;317(25):1565–1570.
17. Bernard GR, et al. A trial of antioxidants N-acetylcysteine and procysteine in ARDS. The Antioxidant in ARDS Study Group. *Chest*. 1997;112(1):164–172.
18. Fan E, Brodie D, Slutsky AS. Acute respiratory distress syndrome: advances in diagnosis and treatment. *JAMA*. 2018;319(7):698–710.
19. Tremblay L, Valenza F, Ribeiro SP, Li J, Slutsky AS. Injurious ventilatory strategies increase cytokines and c-fos m-RNA expression in an isolated rat lung model. *J Clin Invest*. 1997;99(5):944–952.
20. Parsons PE, et al. Lower tidal volume ventilation and plasma cytokine markers of inflammation in patients with acute lung injury. *Crit Care Med*. 2005;33(1):1–6.
21. Izbicki G, Segel MJ, Christensen TG, Conner MW, Breuer R. Time course of bleomycin-induced lung fibrosis. *Int J Exp Pathol*. 2002;83(3):111–119.
22. Chaudhary NI, Schnapp A, Park JE. Pharmacologic differentiation of inflammation and fibrosis in the rat bleomycin model. *Am J Respir Crit Care Med*. 2006;173(7):769–776.
23. Matute-Bello G, Frevert CW, Martin TR. Animal models of acute lung injury. *Am J Physiol Lung Cell Mol Physiol*. 2008;295(3):L379–L399.
24. Mouratis MA, Aidinis V. Modeling pulmonary fibrosis with bleomycin. *Curr Opin Pulm Med*. 2011;17(5):355–361.
25. Gasse P, et al. IL-1R1/MyD88 signaling and the inflammasome are essential in pulmonary inflammation and fibrosis in mice. *J Clin Invest*. 2007;117(12):3786–3799.
26. Misharin AV, Morales-Nebreda L, Mutlu GM, Budinger GR, Perlman H. Flow cytometric analysis of macrophages and dendritic cell subsets in the mouse lung. *Am J Respir Cell Mol Biol*. 2013;49(4):503–510.
27. Gibbons MA, et al. Ly6Chi monocytes direct alternatively activated profibrotic macrophage regulation of lung fibrosis. *Am J Respir Crit Care Med*. 2011;184(5):569–581.
28. Wynn TA, Vannella KM. Macrophages in tissue repair, regeneration, and fibrosis. *Immunity*. 2016;44(3):450–462.
29. D'Alessio FR, et al. $CD4^+CD25^+Foxp3^+$ Tregs resolve experimental lung injury in mice and are present in humans with acute lung injury. *J Clin Invest*. 2009;119(10):2898–2913.
30. Misharin AV, et al. Monocyte-derived alveolar macrophages drive lung fibrosis and persist in the lung over the life span. *J Exp Med*. 2017;214(8):2387–2404.
31. Klune JR, Dhupar R, Cardinal J, Billiar TR, Tsung A. HMGB1: endogenous danger signaling. *Mol Med*. 2008;14(7-8):476–484.
32. Hirsiger S, Simmen HP, Werner CM, Wanner GA, Rittirsch D. Danger signals activating the immune response after trauma. *Mediators Inflamm*. 2012;2012:315941.
33. Namas RA, et al. Insights into the role of chemokines, damage-associated molecular patterns, and lymphocyte-derived mediators from computational models of trauma-induced inflammation. *Antioxid Redox Signal*. 2015;23(17):1370–1387.
34. Matta BM, Reichenbach DK, Blazar BR, Turnquist HR. Alarmins and their receptors as modulators and indicators of alloimmune responses. *Am J Transplant*. 2017;17(2):320–327.
35. Liew FY, Girard JP, Turnquist HR. Interleukin-33 in health and disease. *Nat Rev Immunol*. 2016;16(11):676–689.
36. Marvie P, et al. Interleukin-33 overexpression is associated with liver fibrosis in mice and humans. *J Cell Mol Med*. 2010;14(6B):1726–1739.
37. Manetti M, et al. The IL1-like cytokine IL33 and its receptor ST2 are abnormally expressed in the affected skin and visceral organs of patients with systemic sclerosis. *Ann Rheum Dis*. 2010;69(3):598–605.
38. Molofsky AB, Savage AK, Locksley RM. Interleukin-33 in tissue homeostasis, injury, and inflammation. *Immunity*. 2015;42(6):1005–1019.
39. Martin NT, Martin MU. Interleukin 33 is a guardian of barriers and a local alarmin. *Nat Immunol*. 2016;17(2):122–131.
40. Arpaia N, et al. A Distinct function of regulatory T cells in tissue protection. *Cell*. 2015;162(5):1078–1089.
41. Siede J, et al. IL-33 receptor-expressing regulatory T cells are highly activated, Th2 biased and suppress CD4 T cell proliferation

through IL-10 and TGFβ release. *PLoS ONE*. 2016;11(8):e0161507.
42. Burzyn D, et al. A special population of regulatory T cells potentiates muscle repair. *Cell*. 2013;155(6):1282–1295.
43. Chen CC, Kobayashi T, Iijima K, Hsu FC, Kita H. IL-33 dysregulates regulatory T cells and impairs established immunologic tolerance in the lungs. *J Allergy Clin Immunol*. 2017;140(5):1351–1363.e7.
44. MacDonald KG, Dawson NA, Huang Q, Dunne JV, Levings MK, Broady R. Regulatory T cells produce profibrotic cytokines in the skin of patients with systemic sclerosis. *J Allergy Clin Immunol*. 2015;135(4):946–.e9.
45. Luzina IG, et al. Interleukin-33 potentiates bleomycin-induced lung injury. *Am J Respir Cell Mol Biol*. 2013;49(6):999–1008.
46. Li D, et al. IL-33 promotes ST2-dependent lung fibrosis by the induction of alternatively activated macrophages and innate lymphoid cells in mice. *J Allergy Clin Immunol*. 2014;134(6):1422–1432.e11.
47. Russo RC, et al. Role of the chemokine receptor CXCR2 in bleomycin-induced pulmonary inflammation and fibrosis. *Am J Respir Cell Mol Biol*. 2009;40(4):410–421.
48. Tsukui T, et al. Qualitative rather than quantitative changes are hallmarks of fibroblasts in bleomycin-induced pulmonary fibrosis. *Am J Pathol*. 2013;183(3):758–773.
49. Arnold L, et al. Inflammatory monocytes recruited after skeletal muscle injury switch into antiinflammatory macrophages to support myogenesis. *J Exp Med*. 2007;204(5):1057–1069.
50. Kuswanto W, et al. Poor repair of skeletal muscle in aging mice reflects a defect in local, interleukin-33-dependent accumulation of regulatory T cells. *Immunity*. 2016;44(2):355–367.
51. Turnquist HR, et al. IL-33 expands suppressive CD11b$^+$ Gr-1(int) and regulatory T cells, including ST2L$^+$ Foxp3$^+$ cells, and mediates regulatory T cell-dependent promotion of cardiac allograft survival. *J Immunol*. 2011;187(9):4598–4610.
52. Matta BM, et al. Peri-alloHCT IL-33 administration expands recipient T-regulatory cells that protect mice against acute GVHD. *Blood*. 2016;128(3):427–439.
53. Kim JM, Rasmussen JP, Rudensky AY. Regulatory T cells prevent catastrophic autoimmunity throughout the lifespan of mice. *Nat Immunol*. 2007;8(2):191–197.
54. Matta BM, et al. IL-33 is an unconventional Alarmin that stimulates IL-2 secretion by dendritic cells to selectively expand IL-33R/ST2$^+$ regulatory T cells. *J Immunol*. 2014;193(8):4010–4020.
55. Delacher M, et al. Genome-wide DNA-methylation landscape defines specialization of regulatory T cells in tissues. *Nat Immunol*. 2017;18(10):1160–1172.
56. Zhu J, Paul WE. Heterogeneity and plasticity of T helper cells. *Cell Res*. 2010;20(1):4–12.
57. Nakayama T, et al. Th2 cells in health and disease. *Annu Rev Immunol*. 2017;35:53–84.
58. Wing K, et al. CTLA-4 control over Foxp3$^+$ regulatory T cell function. *Science*. 2008;322(5899):271–275.
59. Voehringer D, Wu D, Liang HE, Locksley RM. Efficient generation of long-distance conditional alleles using recombineering and a dual selection strategy in replicate plates. *BMC Biotechnol*. 2009;9:69.
60. Walkin L, et al. The role of mouse strain differences in the susceptibility to fibrosis: a systematic review. *Fibrogenesis Tissue Repair*. 2013;6(1):18.
61. Robinson KM, Ramanan K, Clay ME, McHugh KJ, Rich HE, Alcorn JF. Novel protective mechanism for interleukin-33 at the mucosal barrier during influenza-associated bacterial superinfection. *Mucosal Immunol*. 2018;11(1):199–208.
62. Murray PJ, et al. Macrophage activation and polarization: nomenclature and experimental guidelines. *Immunity*. 2014;41(1):14–20.
63. Veglia F, Perego M, Gabrilovich D. Myeloid-derived suppressor cells coming of age. *Nat Immunol*. 2018;19(2):108–119.
64. Ostrand-Rosenberg S, Fenselau C. Myeloid-derived suppressor cells: immune-suppressive cells that impair antitumor immunity and are sculpted by their environment. *J Immunol*. 2018;200(2):422–431.
65. Wills-Karp M, et al. Interleukin-13: central mediator of allergic asthma. *Science*. 1998;282(5397):2258–2261.
66. Lee CG, et al. Interleukin-13 induces tissue fibrosis by selectively stimulating and activating transforming growth factor beta(1). *J Exp Med*. 2001;194(6):809–821.
67. Kaviratne M, et al. IL-13 activates a mechanism of tissue fibrosis that is completely TGF-beta independent. *J Immunol*. 2004;173(6):4020–4029.
68. Fichtner-Feigl S, Strober W, Kawakami K, Puri RK, Kitani A. IL-13 signaling through the IL-13alpha2 receptor is involved in induction of TGF-beta1 production and fibrosis. *Nat Med*. 2006;12(1):99–106.
69. Heredia JE, et al. Type 2 innate signals stimulate fibro/adipogenic progenitors to facilitate muscle regeneration. *Cell*. 2013;153(2):376–388.
70. Bosurgi L, et al. Macrophage function in tissue repair and remodeling requires IL-4 or IL-13 with apoptotic cells. *Science*. 2017;356(6342):1072–1076.
71. Gieseck RL, Wilson MS, Wynn TA. Type 2 immunity in tissue repair and fibrosis. *Nat Rev Immunol*. 2018;18(1):62–76.
72. Lechner AJ, et al. Recruited monocytes and type 2 immunity promote lung regeneration following pneumonectomy. *Cell Stem Cell*. 2017;21(1):120–134.e7.
73. Bruce DW, et al. Type 2 innate lymphoid cells treat and prevent acute gastrointestinal graft-versus-host disease. *J Clin Invest*. 2017;127(5):1813–1825.
74. Highfill SL, et al. Bone marrow myeloid-derived suppressor cells (MDSCs) inhibit graft-versus-host disease (GVHD) via an arginase-1-dependent mechanism that is up-regulated by interleukin-13. *Blood*. 2010;116(25):5738–5747.
75. Proto JD, et al. Regulatory T cells promote macrophage efferocytosis during inflammation resolution. *Immunity*. 2018;49(4):666–677.e6.
76. Panduro M, Benoist C, Mathis D. Tissue Tregs. *Annu Rev Immunol*. 2016;34:609–633.
77. Gomez Perdiguero E, et al. Tissue-resident macrophages originate from yolk-sac-derived erythro-myeloid progenitors. *Nature*. 2015;518(7540):547–551.
78. Fan X, Rudensky AY. Hallmarks of tissue-resident lymphocytes. *Cell*. 2016;164(6):1198–1211.
79. Schiering C, et al. The alarmin IL-33 promotes regulatory T-cell function in the intestine. *Nature*. 2014;513(7519):564–568.
80. Zheng T, et al. Cytokine regulation of IL-13Ralpha2 and IL-13Ralpha1 in vivo and in vitro. *J Allergy Clin Immunol*. 2003;111(4):720–728.

81. Bonfield TL, Konstan MW, Berger M. Altered respiratory epithelial cell cytokine production in cystic fibrosis. *J Allergy Clin Immunol*. 1999;104(1):72–78.
82. Fischäder G, Röder-Stolinski C, Wichmann G, Nieber K, Lehmann I. Release of MCP-1 and IL-8 from lung epithelial cells exposed to volatile organic compounds. *Toxicol In Vitro*. 2008;22(2):359–366.
83. Saba S, Soong G, Greenberg S, Prince A. Bacterial stimulation of epithelial G-CSF and GM-CSF expression promotes PMN survival in CF airways. *Am J Respir Cell Mol Biol*. 2002;27(5):561–567.
84. Karo-Atar D, et al. A protective role for IL-13 receptor α 1 in bleomycin-induced pulmonary injury and repair. *Mucosal Immunol*. 2016;9(1):240–253.
85. D'Alessio FR, et al. Enhanced resolution of experimental ARDS through IL-4-mediated lung macrophage reprogramming. *Am J Physiol Lung Cell Mol Physiol*. 2016;310(8):L733–L746.
86. Ito M, et al. Brain regulatory T cells suppress astrogliosis and potentiate neurological recovery. *Nature*. 2019;565(7738):246–250.
87. Noble PW, Barkauskas CE, Jiang D. Pulmonary fibrosis: patterns and perpetrators. *J Clin Invest*. 2012;122(8):2756–2762.
88. Préfontaine D, et al. Increased expression of IL-33 in severe asthma: evidence of expression by airway smooth muscle cells. *J Immunol*. 2009;183(8):5094–5103.
89. Pichery M, et al. Endogenous IL-33 is highly expressed in mouse epithelial barrier tissues, lymphoid organs, brain, embryos, and inflamed tissues: in situ analysis using a novel Il-33-LacZ gene trap reporter strain. *J Immunol*. 2012;188(7):3488–3495.
90. Byers DE, et al. Long-term IL-33-producing epithelial progenitor cells in chronic obstructive lung disease. *J Clin Invest*. 2013;123(9):3967–3982.
91. Kearley J, et al. Cigarette smoke silences innate lymphoid cell function and facilitates an exacerbated type I interleukin-33-dependent response to infection. *Immunity*. 2015;42(3):566–579.
92. Xu J, et al. IL33-mediated ILC2 activation and neutrophil IL5 production in the lung response after severe trauma: A reverse translation study from a human cohort to a mouse trauma model. *PLoS Med*. 2017;14(7):e1002365.
93. Hrusch CL, et al. ICOS protects against mortality from acute lung injury through activation of IL-5$^+$ ILC2s. *Mucosal Immunol*. 2018;11(1):61–70.
94. Bessa J, et al. Altered subcellular localization of IL-33 leads to non-resolving lethal inflammation. *J Autoimmun*. 2014;55:33–41.
95. Jones SA, Scheller J, Rose-John S. Therapeutic strategies for the clinical blockade of IL-6/gp130 signaling. *J Clin Invest*. 2011;121(9):3375–3383.
96. Le TT, et al. Blockade of IL-6 trans signaling attenuates pulmonary fibrosis. *J Immunol*. 2014;193(7):3755–3768.
97. Tadokoro T, Wang Y, Barak LS, Bai Y, Randell SH, Hogan BL. IL-6/STAT3 promotes regeneration of airway ciliated cells from basal stem cells. *Proc Natl Acad Sci USA*. 2014;111(35):E3641–E3649.
98. Liang J, et al. Hyaluronan and TLR4 promote surfactant-protein-C-positive alveolar progenitor cell renewal and prevent severe pulmonary fibrosis in mice. *Nat Med*. 2016;22(11):1285–1293.
99. Campbell IK, et al. Therapeutic targeting of the G-CSF receptor reduces neutrophil trafficking and joint inflammation in antibody-mediated inflammatory arthritis. *J Immunol*. 2016;197(11):4392–4402.
100. Maus UA, et al. Monocytes are potent facilitators of alveolar neutrophil emigration during lung inflammation: role of the CCL2-CCR2 axis. *J Immunol*. 2003;170(6):3273–3278.
101. Kreisel D, et al. In vivo two-photon imaging reveals monocyte-dependent neutrophil extravasation during pulmonary inflammation. *Proc Natl Acad Sci USA*. 2010;107(42):18073–18078.
102. Baran CP, et al. Important roles for macrophage colony-stimulating factor, CC chemokine ligand 2, and mononuclear phagocytes in the pathogenesis of pulmonary fibrosis. *Am J Respir Crit Care Med*. 2007;176(1):78–89.
103. Rosseau S, et al. Phenotypic characterization of alveolar monocyte recruitment in acute respiratory distress syndrome. *Am J Physiol Lung Cell Mol Physiol*. 2000;279(1):L25–L35.
104. Liang J, et al. A macrophage subpopulation recruited by CC chemokine ligand-2 clears apoptotic cells in noninfectious lung injury. *Am J Physiol Lung Cell Mol Physiol*. 2012;302(9):L933–L940.
105. Ashbaugh DG, Bigelow DB, Petty TL, Levine BE. Acute respiratory distress in adults. *Lancet*. 1967;2(7511):319–323.
106. Oboki K, et al. IL-33 is a crucial amplifier of innate rather than acquired immunity. *Proc Natl Acad Sci USA*. 2010;107(43):18581–18586.
107. Townsend MJ, Fallon PG, Matthews DJ, Jolin HE, McKenzie AN. T1/ST2-deficient mice demonstrate the importance of T1/ST2 in developing primary T helper cell type 2 responses. *J Exp Med*. 2000;191(6):1069–1076.
108. Fan MH, et al. Fibroblast activation protein (FAP) accelerates collagen degradation and clearance from lungs in mice. *J Biol Chem*. 2016;291(15):8070–8089.